© 2014. Published by The Company of Biologists Ltd | Journal of Cell Science (2014) 127, 5115–5125 doi:10.1242/jcs.161133

RESEARCH ARTICLE

Signaling in chemotactic amoebae remains spatially confined to stimulated membrane regions

Matthias Gerhardt, Michael Walz and Carsten Beta*

ABSTRACT

Recent work has demonstrated that the receptor-mediated signaling system in chemotactic amoeboid cells shows typical properties of an excitable system. Here, we delivered spatially confined stimuli of the chemoattractant cAMP to the membrane of differentiated *Dictyostelium discoideum* cells to investigate whether localized receptor stimuli can induce the spreading of excitable waves in the G-protein-dependent signal transduction system. By imaging the spatiotemporal dynamics of fluorescent markers for phosphatidylinositol (3,4,5)-trisphosphate (PIP_3), PTEN and filamentous actin, we observed that the activity of the signaling pathway remained spatially confined to the stimulated membrane region. Neighboring parts of the membrane were not excited and no receptor-initiated spatial spreading of excitation waves was observed. To generate localized cAMP stimuli, either particles that carried covalently bound cAMP molecules on their surface were brought into contact with the cell or a patch of the cell membrane was aspirated into a glass micropipette to shield this patch against freely diffusing cAMP molecules in the surrounding medium. Additionally, the binding site of the cAMP receptor was probed with different surface-immobilized cAMP molecules, confirming results from earlier ligand-binding studies.

KEY WORDS: Signal transduction, Excitable dynamics, *Dictyostelium*, cAMP, PIP_3, PIP_2, PI3K, PTEN, Micropipette aspiration, cAMP receptor, Patch clamp

INTRODUCTION

In many cases, the amoeboid movement of cells is guided by chemical gradients in the concentration of extracellular signaling agents (Ridley et al., 2003). This process, generally referred to as chemotaxis, plays an important role in various biological processes, including wound healing, the spreading of infections and cancer metastasis (Friedl and Gilmour, 2009). A G-protein-coupled receptor (GPR) senses the chemoattractant and triggers intracellular signaling cascades that initiate cytoskeletal rearrangements and, ultimately, directed cell movement (Swaney et al., 2010). Many details of the chemotactic mechanism, including components of the signaling pathway that interconnects the GPR and the actin cytoskeleton of the cell are conserved between *Dictyostelium discoideum* and mammalian cells, making the amoeba a popular model for studying chemotactic signaling in eukaryotes (Annesley and Fisher, 2009; Kölsch et al., 2008; Prabhu and Eichinger, 2006).

In starvation-developed *Dictyostelium* cells, the initial chemoattractant sensing is mediated by the GPRs cAR1 and, to a lesser extent, cAR3 (Insall et al., 1994) that are activated by extracellular cyclic AMP (cAMP). Upon a ligand-binding event, the heterotrimeric G protein Gαβγ dissociates into the Gα and the Gβγ subclusters (Janetopoulos et. al., 2001; Xu et. al., 2005), a process that mainly takes place inside or close to the cell membrane (Elzie et. al., 2009). Photobleaching experiments suggest that active and inactive G proteins cycle between the plasma membrane and a cytosolic pool, such that receptor stimulation enhances membrane localization of the Gα subunit (Elzie et. al., 2009). Dissociation of the heterotrimeric G protein triggers Ras guanine nucleotide exchange factors (GEFs) that catalyze the transition from inactive GDP-loaded Ras to active Ras–GTP (Sasaki et al., 2004; Kae et al., 2007). Recently, Ras activation was shown to undergo three distinct phases – initial activation, symmetry breaking and confinement (Kortholt et al., 2013). The initial activation is proportional to the extracellular cAMP concentration and is mediated by Gβγ, whereas subsequent strong symmetry breaking of the intracellular Ras activation in the gradient direction crucially depends on Gα. For the Gα subunit, a nonreceptor GEF has been identified that amplifies Gα-dependent symmetry breaking during chemotaxis (Kataria et al., 2013).

Ras triggers activity of the evolutionarily conserved class 1b phosphoinositide 3-kinase (PI3K) that produces phosphatidylinositol (3,4,5)-trisphosphate (PIP_3) from phosphatidylinositol 4,5-bisphosphate (PIP_2), accompanied by a loss of the phosphoinositide 3-phosphatase (PTEN) from the membrane. PTEN can exist either in an activated or in an inactivated state (Rahdar et al., 2009) and is the PIP_3-degrading enzyme that converts PIP_3 into PIP_2. Besides activation mediated by Ras (Kortholt et al., 2013), the class 1b PI3Ks also have a binding site for the Gβγ subcluster, which has been identified in different mammalian systems (Krugmann et al., 2002; Brock et al., 2003; Suire et al., 2005). Once activated, PI3K begins to synthesize PIP_3, which is a second messenger to activate further downstream signaling (Stein and Waterfield, 2000), such as WASP interaction with Arp2/3 to initiate actin polymerization (Pantaloni et al., 2001).

In gradients of cAMP, PIP_3 accumulates at the leading edge of the cell, whereas the membrane at the sides and at the back is enriched in PIP_2. Even though gradient sensing and chemotaxis do not depend on PIP_3 signaling alone (Hoeller and Kay, 2007), PI3K activity is essential for orientation in shallow gradients (Postma et al., 2004; Takeda et al., 2007) and consistently occurs in many different chemotactic cell types. The gradient-induced symmetry breaking in the phosphoinositide distribution has inspired numerous gradient-sensing models. The most widely used model involves a local activator and a fast-diffusing global inhibitor — the 'local excitation, global inhibition' (LEGI) model

Institute of Physics and Astronomy, University of Potsdam, Karl-Liebknecht-Strasse 24/25, 14476 Potsdam, Germany.

*Author for correspondence (beta@uni-potsdam.de)

Received 6 August 2014; Accepted 25 September 2014

Journal of Cell Science (2014) 127, 5115–5125 doi:10.1242/jcs.161133

(Parent and Devreotes, 1999; Levchenko and Iglesias, 2002). Different variants of this model have been explored (see for example Levine et al., 2006; Beta et al., 2008; Xiong et al., 2010; Takeda et al., 2012).

Recent imaging studies have demonstrated that PIP_3-rich membrane regions might self-organize into coherent wave-like domains that travel across the cell membrane (Gerisch et al., 2012). There is evidence that these waves are instrumental for particle uptake during phagocytosis (Gerisch et al., 2009). Furthermore, based on its phosphoinositide composition, the wave territory has been found to relate to the front region and the area not covered by the wave to the tail region of a cell undergoing chemotaxis (Gerisch et al., 2012). The PIP_3-rich domains move in conjunction with actin waves at their border and show the hallmarks of waves in an excitable system, such as mutual annihilation upon collision or spiral core formation (Gerisch et al., 2009; Gerisch et al., 2011; Taniguchi et al., 2013; Gerhardt et al., 2014). Also, oscillatory dynamics has been observed (Westendorf et al., 2013; Huang et al., 2013). Prompted by these observations, recent modeling approaches rely on excitable dynamics to describe gradient sensing and chemotaxis (Xiong et al., 2010; Hecht et al., 2011; Neilson et al., 2011; Cooper et al., 2012; Huang et al., 2013; Knoch et al., 2014). To what extent is this mechanism supported by experimental observations?

The propagation of excitable waves requires a spatially extended active medium with two distinct properties – (1) each location of the medium exhibits excitable dynamics, i.e. upon a super-threshold perturbation, a transient temporal excitation occurs, followed by a refractory period; (2) due to spatial coupling between adjacent elements of the medium, a local excitation induces a super-threshold perturbation also at neighboring locations, so that the excitation spreads as a wave through the active medium. Recent experimental results support condition 1 by showing that cells exposed to uniform cAMP stimuli indeed exhibit threshold-type behavior and a refractory period for the temporal dynamics of both Ras-binding domain (RBD) translocation and PIP_3 formation (Huang et al., 2013; Nishikawa et al., 2014). Furthermore, the observation of spontaneous wave patterns supports condition 2. But can we also initiate wave patterns similar to the spontaneously emerging PIP_3 and actin waves by a confined, localized cAMP receptor stimulus?

In this study, we developed two alternative tools to deliver localized cAMP stimuli to confined membrane regions of chemotactic *Dictyostelium* cells, in order to explore whether spreading excitation waves can be initiated by the receptor pathway. We probed excitability of the signal transduction system in response to cAMP receptor stimulation based on the production of PIP_3 by PI3K, the degradation of PIP_3 by PTEN and the polymerization of actin. The fluorescent markers we used to image the excitation process were the PH_{CRAC}–GFP fusion protein to detect PIP_3 (Parent et al., 1998), the PTEN–GFP fusion protein to study the spatiotemporal dynamics of PTEN (Iijima and Devreotes, 2002; Funamoto et al., 2002; Gerisch et al., 2012) and DdLimEΔ–RFP to detect filamentous actin (Schneider et al., 2003). Our data show that no spreading excitation waves are initiated in response to a localized receptor stimulus.

RESULTS

To test whether receptor-induced excitations in the chemotactic signal transduction network of *Dictyostelium* can spread along the cell membrane, we developed two different methods to stimulate a confined membrane area of a differentiated *Dictyostelium* cell. On the one hand, we used Sepharose particles that carried covalently immobilized cAMP molecules on their surface to stimulate a confined area of the cell membrane. On the other hand, to also stimulate confined membrane areas with freely diffusing cAMP molecules, we furthermore developed a patch-clamp-based technique that allowed us to locally shield a patch of the cell membrane against cAMP molecules from the extracellular medium. During stimulation, we imaged the intracellular distribution of fluorescent markers for PIP_3, PTEN and F-actin and compared the localization of these proteins at the stimulated and non-stimulated sites of the cell membrane.

PIP_3 pattern in response to a localized receptor stimulus initiated by surface-immobilized cAMP molecules (particle-based stimulation)

We studied the receptor-mediated PIP_3-response in starvation-developed *Dictyostelium* cells that were brought into contact with Sepharose particles decorated with covalently immobilized cAMP molecules on their surface. Particles with four different linker types were tested that exposed the cAMP molecules in different configurations on their surface – 8-AH-cAMP, 6-AH-cAMP, 2-AH-cAMP and 2′O-AHC-cAMP (supplementary material Fig. S1). The mean particle diameter was 100 µm, and the concentration of cAMP molecules immobilized on the particles was on the order of 6 µmol/ml. In the first series of tests, particles with the different cAMP coatings were sedimented onto a layer of differentiated *Dictyostelium* cells that expressed PH_{CRAC}–GFP, a marker that binds to PIP_3-rich regions in the cell membrane (Parent et al., 1998). We continuously imaged the intracellular PH_{CRAC}–GFP distribution while the particles were coming into contact with the adherent cells. Finally, a small volume (20 µl) of cAMP solution was added to the extracellular medium as a control to verify that the cells were indeed responsive to extracellular cAMP. The concentration of the added cAMP solution corresponded to a final value of 20 µM in the well-mixed case. Note that owing to the ongoing mixing process in the culture dish, the initial cAMP stimulus received by the cells was much lower than the final value (see the Discussion for a detailed concentration estimate). Out of the four cAMP coatings tested, only particles with cAMP molecules linked in the 6-AH-cAMP configuration reliably triggered a translocation of PH_{CRAC}–GFP from the cytosol to the membrane after collision with cells (supplementary material Fig. S2). We furthermore observed that in cases where only parts of the cell membrane were excited by contact with a cAMP-coated particle, the remaining parts of the cell membrane were less responsive to the subsequent global cAMP stimulus. Two examples of this behavior are displayed in supplementary material Movies 3 and 4. Note also that we observed an inhibitory effect for the 2′O-AHC-cAMP ligand, as subsequent addition of cAMP did not trigger any PH_{CRAC}–GFP translocation in this case (supplementary material Fig. S2).

In the second series of experiments, Sepharose particles with 6-AH-cAMP ligands were used to investigate the contact-induced PH_{CRAC}–GFP translocation in more detail. In addition to the cAMP coating, the particles were stained with Rhodamine for confocal imaging of the particle surface. A 6-AH-cAMP-coated and Rhodamine-stained particle was impaled on a glass micropipette that was mounted on the head of a micromanipulator. Using the micromanipulator, the particle was moved towards a differentiated

Journal of Cell Science (2014) 127, 5115–5125 doi:10.1242/jcs.161133

Dictyostelium cell and gently brought into contact with the cell membrane. The contact event was imaged using the *Z*-stack mode of the laser-scanning confocal microscope. We recorded at two different excitation wavelengths to capture the fluorescence signal of the PH_{CRAC}–GFP marker (green) and that of the Rhodamine-stained particle surface (red) at the same time.

After the particle and the cell surfaces came into contact, translocation of the PH_{CRAC}–GFP marker to the membrane was observed. Remarkably, only the membrane area that was in direct contact with the particle surface was decorated with PH_{CRAC}–GFP. At the end of the contact zone, the fluorescence intensity decreased abruptly (Fig. 1). We performed control experiments with particles that did not carry any cAMP coating at their surface to test whether the localized translocation of the PH_{CRAC}–GFP marker was triggered by the mechanical impact of the approaching particle. No PH_{CRAC}–GFP translocation was observed (Fig. 2). This clearly indicates that the localized PH_{CRAC}–GFP signal in Fig. 1 can be attributed to a receptor response induced by the 6-AH-cAMP coating of the particle. The PH_{CRAC}–GFP translocation initiated by the surface-immobilized cAMP ligands was similarly strong as translocations triggered by freely diffusing cAMP.

PIP_3 pattern in response to a localized receptor stimulus initiated by freely diffusing cAMP molecules (patch clamp shielding)

Particles that expose cAMP ligands at their surface induce a localized PH_{CRAC}–GFP translocation when brought into contact with the membrane of a differentiated *Dictyostelium* cell. In order to test whether localized stimuli with free cAMP molecules induce a similar translocation pattern, we developed a method based on classical patch clamp techniques that allowed us to shield a membrane region against cAMP molecules in the extracellular medium. A patch of the membrane of a differentiated *Dictyostelium* cell was aspirated into the open tip of a glass pipette with an open resistivity between 2 and 4 MΩ. Depending on the pressure inside the pipette, the seal resistivity could be adjusted between 4 MΩ and values >100 MΩ.

Brightfield microscopy images clearly show the bulb-shaped membrane invagination inside the glass pipette (Fig. 3B). The membrane patch inside the pipette is readily accessible for fluorescence imaging by laser-scanning confocal microscopy to reveal the distribution of intracellular markers at the membrane because the excitation plane is intersecting the patch inside the glass pipette as well as the remaining cell in the extracellular medium. Depending on the position of the excitation plane, this might cause the membrane of the shielded patch and the remaining cell body to appear as two disconnected circular regions (see Fig. 3C for an explanatory schematic view).

It can be expected that for sufficiently high seal resistivities, small molecules like cAMP can no longer penetrate into the opening of the pipette. In this case, the addition of cAMP to the surrounding medium will stimulate the receptors at the entire cell surface except for the part of the membrane inside the pipette. We performed a series of aspiration experiments with PH_{CRAC}–GFP-expressing *Dictyostelium* cells in which the seal resistivity was successively increased from 4 MΩ to ~100 MΩ. For resistivities <50 MΩ, the addition of cAMP to the surrounding medium induced a translocation of the PH_{CRAC}–GFP marker to all parts of the cell membrane, including the membrane patch inside the glass pipette (Fig. 4A). If the seal resistivity was adjusted to >50 MΩ, no PH_{CRAC}–GFP translocation to the membrane inside the glass pipette was observed, whereas the remaining membrane outside the pipette was still decorated with the fluorescent marker upon cAMP stimulation (Fig. 4B; supplementary material Fig. S3). We thus conclude that for resistivities >50 MΩ, the seal between the glass pipette and the membrane is strong enough to prevent cAMP molecules from entering into the pipette tip, so that the membrane patch inside the pipette is shielded against the cAMP stimulus. In all cases, cells were stimulated with a final cAMP concentration of 20 µM. We note, however, that the initial stimulus was much weaker than this, see also the comment above and the Discussion.

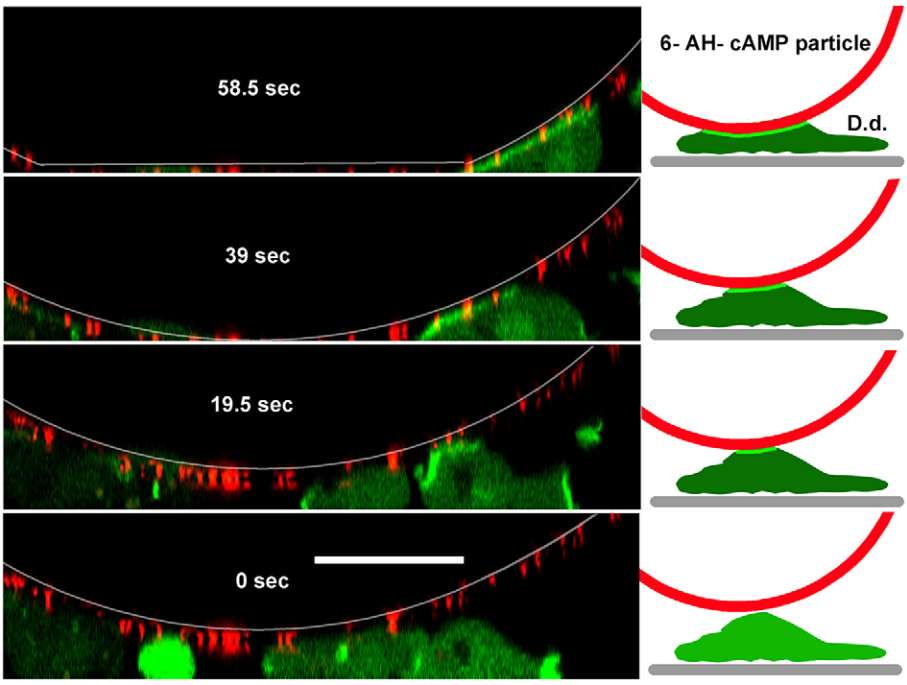

Fig. 1. Stimulation with cAMP-coated micro-particles. An impaled Sepharose micro-particle that is exposing covalently bound cAMP molecules (6-AH-cAMP) on its surface was brought into contact with a differentiated *Dictyostelium* cell (D.d.) expressing the PIP_3 marker PH_{CRAC}–GFP (green). For better visibility, the surface of the particle was stained with Rhodamine (red). After contact with the particle, the enhanced fluorescence at the inner cell membrane indicates a PH_{CRAC}–GFP decoration and thus the presence of PIP_3. Images are taken 19.5 s apart. Scale bar: 10 µm.

Journal of Cell Science (2014) 127, 5115–5125 doi:10.1242/jcs.161133

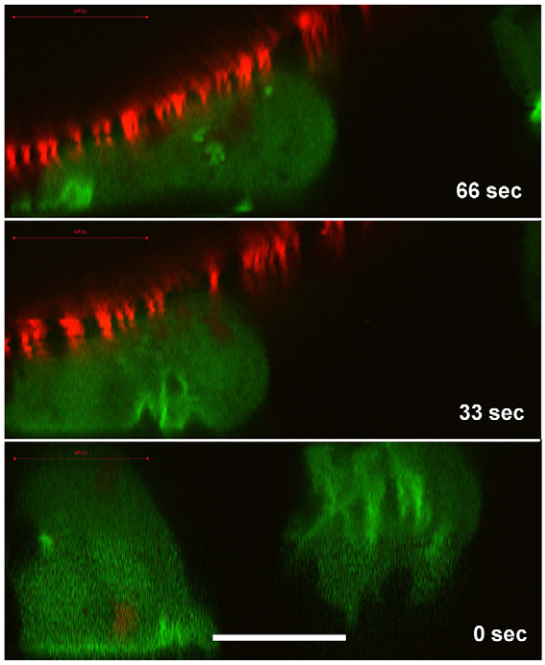

Fig. 2. Mechanical stimulation with micro-particles (control). A Sepharose particle that did not carry any cAMP molecules on its surface was brought into contact with a differentiated *Dictyostelium* cell that expresses the PIP_3 marker PH_{CRAC}–GFP (green). The surface of the particle is indicated by red fluorescence of the Rhodamine (red), which was used to stain the particle. Upon contact between the particle and the cell between 33 and 66 s, the intensity of green fluorescence in the membrane area in contact with the particle did not change. Scale bar: 10 μm.

Similar to the results obtained by stimulation with cAMP-coated particles, the zone of PH_{CRAC}–GFP localization was clearly confined to membrane areas that were in direct contact with cAMP on the outside of the cell and ended abruptly with the beginning of the shielded region inside the glass pipette where no cAMP was present (note that the seal is not necessarily established at the tip but might be located further inside the pipette). Up to 12.5 s after addition of cAMP, the seal resistivity was kept constant and the fluorescence at the unshielded cell membrane as well as at the shielded patch inside the pipette was observed. For all experiments with a seal resistivity >50 MΩ, a steep transition zone of PH_{CRAC}–GFP marker localization remained between the membrane region exposed to cAMP and that which was shielded against cAMP.

PTEN and actin patterns in response to a localized stimulus with freely diffusing cAMP molecules (patch clamp shielding)

Besides the translocation pattern of the PH_{CRAC}–GFP marker, we also studied the response of the PIP_3-degrading phosphatase PTEN and of the actin system. We performed aspiration experiments as described in the previous section, now using a differentiated *Dictyostelium* cell line that simultaneously expressed PTEN–GFP and DdLimEΔ–RFP, a marker for filamentous actin. Based on the results shown in Fig. 5, we could compare the localization of PTEN and F-actin at the open and shielded parts of the cell membrane following cAMP stimulation. At the open membrane that was in direct contact with cAMP during stimulation, the PTEN decoration vanished rapidly while the cortical LimEΔ localization reached its maximum. However, at the shielded membrane patch inside the pipette, the PTEN decoration stayed intact after cAMP stimulation and the LimEΔ signal did not change. To quantify the fluorescence

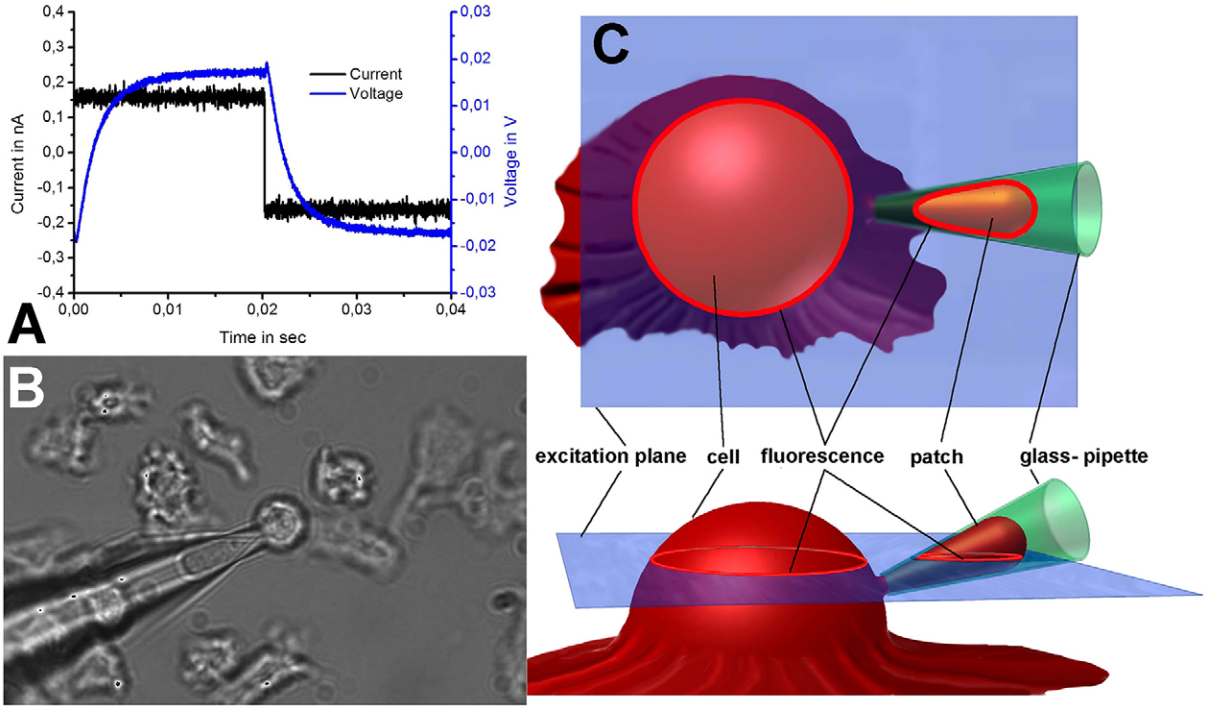

Fig. 3. Patch-clamp shielding experiment. (A) Pulse protocol in the I-clamp mode for measuring the seal resistivity, using an AxoPatch 200B amplifier. The current command was set to 160 pA (duty cycle 50%), causing a voltage maximum amplitude of 17 mV. In the given example, the direct current seal resistivity approached 106 MΩ. (B) Bright-field view of a patch-clamped cell. (C) Schematic view of the micropipette aspiration experiment. For confocal fluorescence imaging, the cell of interest (red) is intersected by the focal plane of a microscope (blue). A patch of the cell membrane is aspirated into a glass pipette (green) that is also intersected by the imaging plane, so that a fraction of the cell membrane and of the patch inside the pipette is imaged at the same time.

Journal of Cell Science (2014) 127, 5115–5125 doi:10.1242/jcs.161133

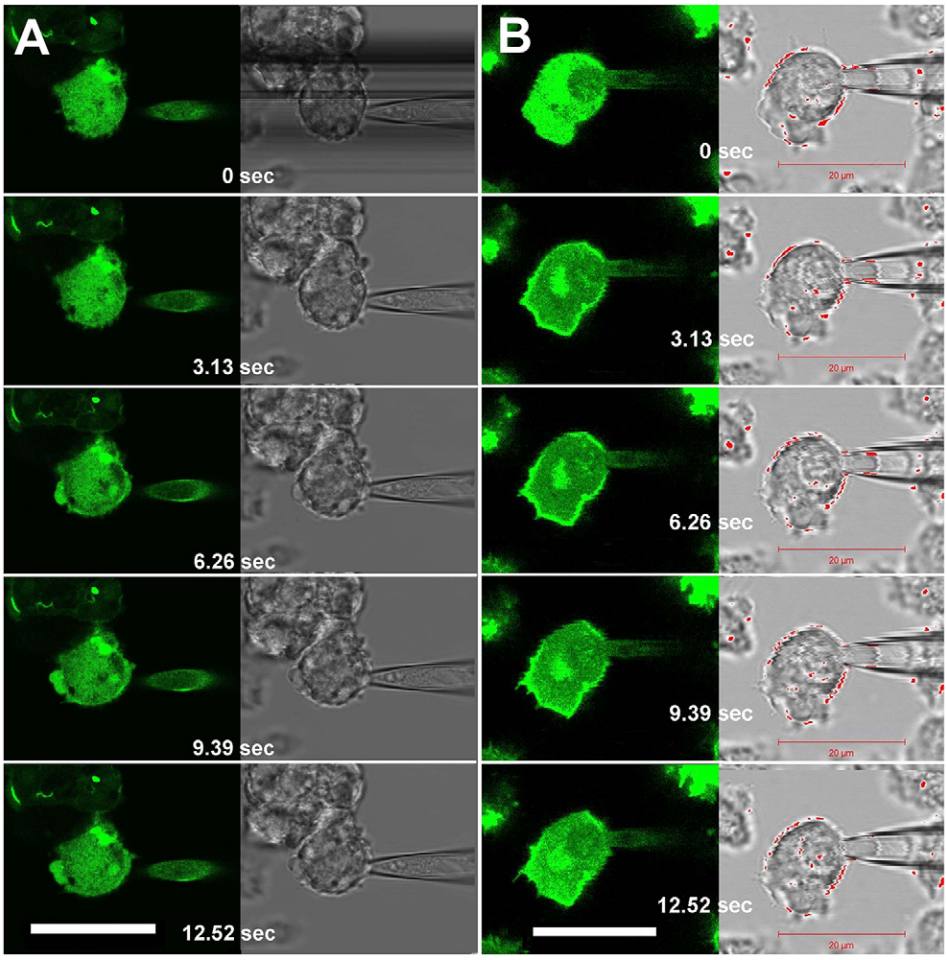

Fig. 4. Shielding of a membrane patch by micropipette aspiration. A differentiated PH_{CRAC}–GFP-expressing *Dictyostelium* cell was imaged at an excitation wavelength of 488 nm to visualize localization of the PIP_3 marker. Simultaneously, brightfield images were recorded to visualize the glass pipette in contact with the cell under investigation. (A) After adjusting the seal resistivity to <50 MΩ, 20 µM cAMP was added to the surrounding medium. The translocation of the PH_{CRAC}–GFP marker, also inside the glass pipette, was clearly detectable. (B) The same experiment was repeated with a seal resistivity >50 MΩ. No PH_{CRAC}–GFP translocation occurred at the membrane inside the pipette. In both cases, frames are 3.13 s apart. The time-point of cAMP addition is indicated by a shadow in the brightfield image (top left), resulting from a partial interruption of the light path by the pipette.

intensities at the cell membrane exposed to cAMP and at the shielded patch, an image analysis tool was developed to average the intensity profile in a direction normal to the cell membrane along the perimeter of the cell (see Materials and Methods).

The quantitative analysis of the PTEN–GFP fluorescence signal confirmed that the PTEN localization vanished at the cAMP-exposed membrane areas and stayed constant at the shielded membrane (Fig. 6). Similarly, the DdLimEΔ–RFP marker showed a response in the cortical areas adjacent to the cAMP-exposed membrane and remained unchanged at the shielded areas (Fig. 6). Further examples demonstrating that no DdLimEΔ–RFP translocation takes place in the shielded parts of the cell as can be seen in Fig. 7.

Note that throughout the experiment, an increased DdLimEΔ–RFP localization was found inside the pipette close to the tip (Fig. 7), as reported previously (Luo et al., 2013). We conjecture that this F-actin accumulation is caused by the mechanical stress exerted by the pipette tip. To test this hypothesis, we mechanically stimulated a cell by touching its surface with the tip of a glass pipette (supplementary material Fig. S4A). Indeed, we observed that, at the site of contact with the pipette tip, the DdLimEΔ–RFP fluorescence initially increased significantly but decreased later, whereas the distribution of the PTEN–GFP marker remained largely unchanged.

DISCUSSION

In this study, we investigated whether localized cAMP receptor stimuli can trigger spreading excitation waves in the signal transduction network of differentiated *Dictyostelium* cells. We used cell lines expressing fluorescent markers of PIP_3, PTEN and filamentous actin, and we monitored their spatiotemporal responses by laser-scanning confocal microscopy. In contrast to other studies, we applied localized cAMP stimuli that were spatially restricted to a confined membrane area. Such stimuli were either generated by contact with a surface that carried immobilized cAMP molecules or by using a patch clamp technique that allows the shielding of a patch of the cell membrane by micropipette aspiration. The main results of our study are that (1) localized stimulation of the cAMP receptor induced activations in the chemotactic signal transduction network of *Dictyostelium* that remained locally confined to the stimulated membrane region. No wave-like spreading of the excitation along the cell membrane was observed. (2) Previous insights into the ligand-binding site of the cAMP receptor (GPR) are in good agreement with our results.

The cAMP-binding site

Earlier studies have characterized the binding site of the cAMP receptor in *Dictyostelium* using different derivates of the cAMP molecule (Van Haastert and Kien, 1983; Mato et al., 1978). It was found that especially the anti-configuration of the cAMP molecule binds to the receptors through the two hydrogen bonds on the amine at position 6 and on the oxygen at position 3′ (supplementary material Fig. S1). A similar result had been reported earlier, claiming a third hydrogen bond between the receptor-binding site and the amine at position 7 of the purine

Journal of Cell Science (2014) 127, 5115–5125 doi:10.1242/jcs.161133

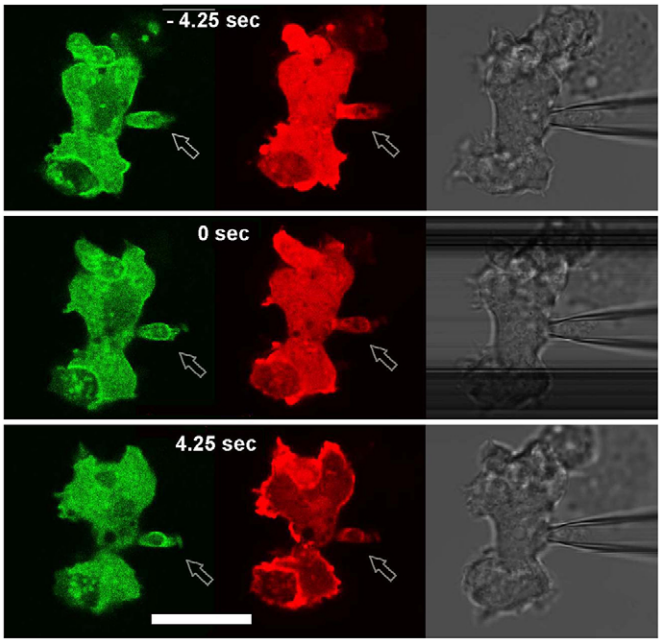

Fig. 5. PTEN and actin dynamics. Shielding of a membrane patch against cAMP stimulation to investigate PTEN–GFP (green) and DdLimEΔ–RFP (red) translocation simultaneously. Upon cAMP stimulation, PTEN–GFP decoration of the cell membrane is lost, except for the shielded part inside the pipette (left). DdLimEΔ–RFP is clearly recruited to the cell cortex and remained unchanged in the shielded part (middle). The time between adjacent frames was 4.25 s, cAMP addition took place at 0 s. Arrows indicate the aspirated membrane patch. Scale bar: 20 μm.

group (Mato et al., 1978). In both cases, it was concluded that ligand binding to the receptor and the triggering of the receptor response are different events that depend on different properties of the ligand. Modified cAMP molecules can cause a response similar to that of cAMP but they can also inhibit the receptor (Van Haastert et al., 1982).

The 6-AH-cAMP [N6-(6-aminohexyl)-adenosine-3′,5′-cyclic monophosphate] used in this study is immobilized on a particle surface through an amine group between the linker and the nitrogen at position 6 of the purine group. According to Van Haastert and Kien, 1983, a modification of this amine influences the binding of this molecule with the receptor. The fact that we nevertheless observed a translocation of the PH_{CRAC}–GFP marker upon collision of a particle carrying 6-AH-cAMP and a *Dictyostelium* cell can be attributed to the high concentration of 6 μmol/ml (6 mM) of surface-bound cAMP ligands that are exposed by these particles. Also, the surface of the Sepharose particles is rough and therefore much larger than the surface of a comparable sphere. We thus conclude that, in our experiments, the reduced binding affinity due to the modification at position 6 of the adenine moiety is compensated for by the much higher ligand concentration. Under these conditions, the fluorescence intensity of the PH_{CRAC}–GFP-decorated membrane in contact with surface-immobilized cAMP was found to be comparable to that of PH_{CRAC}–GFP translocations triggered by freely diffusing cAMP molecules.

Our observations of cellular responses upon contact with 8-AH-cAMP, 2-AH-cAMP and 2′O-AHC-cAMP are in good agreement with the results reported previously (Mato et al., 1978; Van Haastert and Kien, 1983). In particular, Van Haastert et al., 1982 described an inhibitory effect if the cAMP molecule is modified at position 2′ of the ribose. In agreement with this

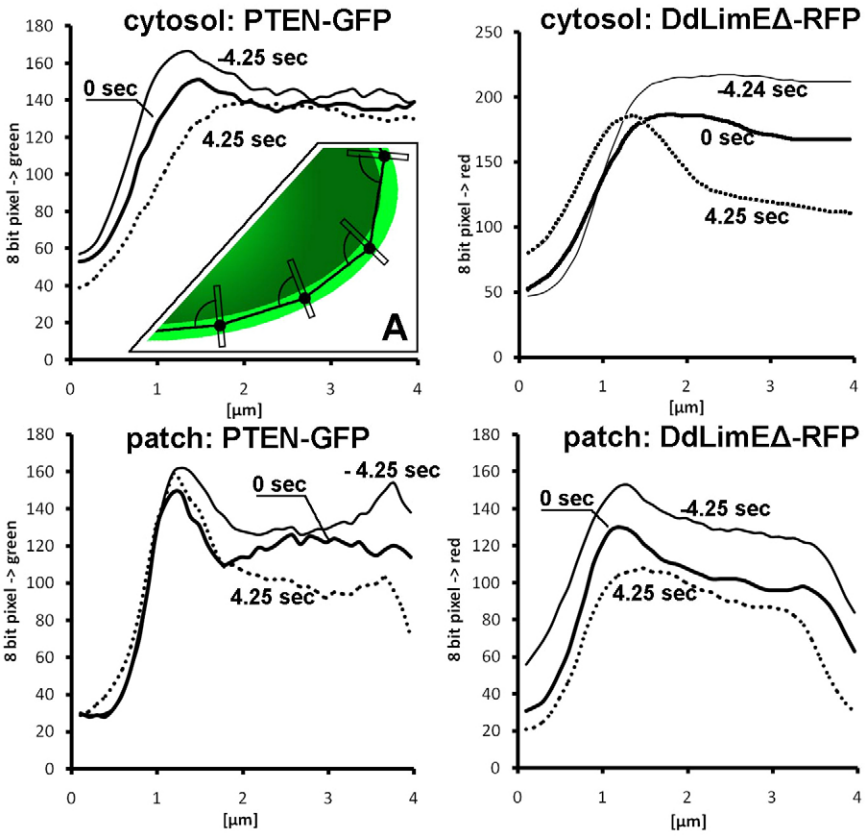

Fig. 6. Quantitative analysis of fluorescence translocation in shielded and unshielded membrane parts. The quantitative image analysis of the unshielded (cytosol, upper row) and shielded regions (patch, lower row) revealed that membrane decoration with PTEN (left) is lost in the unshielded part (upper) and persisted in the shielded part (lower). Cortical LimE localization (right) becomes more pronounced in the unshielded part (upper) and remained constant in the shielded part (lower), except for photobleaching. Data are taken from the PTEN–GFP/DdLimEΔ–RFP-coexpressing cell displayed in Fig. 5. (A) Schematic illustrating how the fluorescence profile was measured at each point of the polygon over a length of 4 μm normal to the cell border.

Journal of Cell Science (2014) 127, 5115–5125 doi:10.1242/jcs.161133

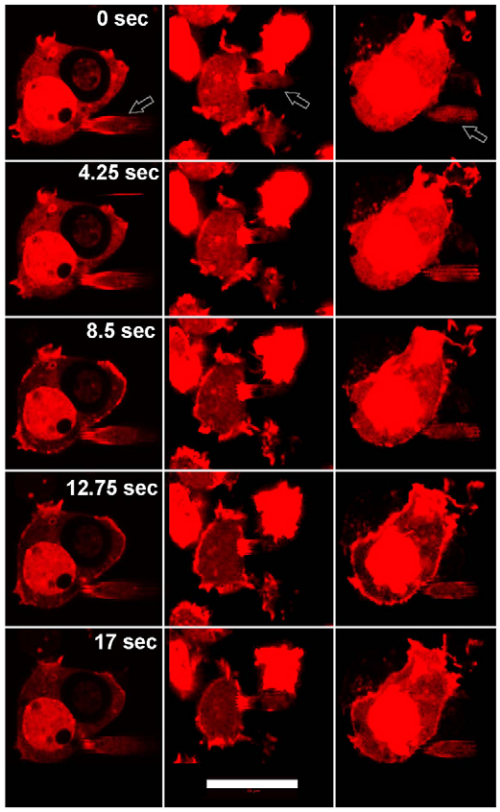

Fig. 7. Actin dynamics in the shielded and unshielded parts of the membrane. Upon cAMP stimulation, DdLimEΔ–RFP (red) is recruited to the cell cortex in the unshielded parts of the cell and remains unchanged in the shielded part. Three independent examples are displayed. The arrows indicate the aspirated membrane patch. Scale bar: 10 µm.

finding, we observed an inhibitory effect of the 2′O-AHC-cAMP upon contact with a cell if free cAMP molecules were subsequently added. The 2′O-AHC-cAMP is immobilized by an amide bound with the oxygen at position 2′ of the ribose.

Response to confined AMP stimuli

We investigated the spatiotemporal dynamics of the cAMP-receptor-mediated signal transduction network in *Dictyostelium* by applying locally confined cAMP stimuli to the membrane of chemotactic cells. The cAMP stimuli were characterized by a step-like concentration profile, where the concentration of cAMP changed from zero to a maximum value over a distance <2 µm, thus allowing us to locally stimulate a confined region of the cell membrane. We explored two different techniques to generate the confined cAMP stimuli.

First, we imaged the contact site between the membrane of PH_{CRAC}–GFP-expressing cells and the surface of particles that expose immobilized cAMP molecules. At the contact site, a translocation of PH_{CRAC}–GFP to the cell membrane was observed, indicating the formation of PIP_3. The translocation of the PH_{CRAC}–GFP marker was clearly confined to the contact area, and the PH_{CRAC}–GFP decoration decreased abruptly where the contact between the cell and the particle ended. Second, we used a more sophisticated method to generate confined cAMP stimuli based on shielding a patch of the cell membrane against freely diffusing cAMP molecules by aspiration into a micropipette. Similar to the clear confinement of the intracellular PH_{CRAC}–GFP decoration to the contact area with cAMP-decorated particles described above, the micropipette aspiration experiment also showed that the PH_{CRAC}–GFP signal is restricted to those membrane areas that are in direct contact with extracellular cAMP. No translocation was observed to the shielded parts of the membrane.

We note that in the current setup, it is technically not possible to directly test the responsiveness of the aspirated membrane by applying cAMP to the shielded parts of the membrane on the inside of the pipette. However, there are strong indications that the membrane inside the pipette remains responsive to cAMP. First, for seal resistivities just below 50 MΩ, the membrane is fully responsive (Fig. 4A). Second, we also note that the so-called loose patch clamp technique allows the measurement of action potentials of ganglion cells at a sealed membrane patch (Stett et al., 2000; Gerhardt et al., 2011). Even though the underlying mechanisms of these processes are very different, this further indicates that signaling at the membrane remains intact during pipette aspiration experiments. Finally, the data displayed in supplementary material Fig. S4B demonstrates that, upon cAMP stimulation, the LimE localization in the seal region at the tip of the pipette increased, clearly highlighting that, even in regions where the mechanical stress is maximal, the membrane is still responsive to cAMP.

At the interface between the shielded and non-shielded parts of the cell membrane, the PH_{CRAC}–GFP fluorescence intensity changed across a narrow transition zone. This transition zone was displayed intracellularly by the fluorescence markers at the edge of the stimulated membrane area. The extension of this transition zone was found to be equal to that of the cAMP gradient at the border of the confined stimulus that corresponds in a first approximation to a step function.

A similar result was also obtained when monitoring the fluorescence intensity of the DdLimEΔ–RFP marker that indicates filamentous actin. The mechanical stress induced by the tip of the micropipette caused an increased fluorescence of the DdLimEΔ–RFP marker even in the absence of cAMP, as reported previously (Luo et al., 2013). However, it was not the case that the complete membrane patch inside the micropipette displayed enhanced DdLimEΔ–RFP fluorescence, but only those parts of the membrane that were under mechanical stress in the region of the seal at the tip of the micropipette. Upon cAMP stimulation, the fluorescence at the membrane in contact with cAMP increased, whereas the intensity at the membrane of the shielded patch remained unchanged. Whether mechanically induced actin polymerization in the seal region between the membrane and the micropipette acts as a border that prevents spatial spreading of actin polymerization remains an open question.

The confined cAMP stimulation was further extended to cells expressing PTEN–GFP. PTEN is localized at PIP_2-rich membrane regions, indicating those parts of the membrane that have been not in contact with extracellular cAMP. Upon cAMP stimulation, PTEN translocates into the cytosol, followed by PIP_3 formation at the membrane (Iijima and Devreotes, 2002; Funamoto et al., 2002). In our localized stimulation experiments, we observed that the fluorescence localization of PTEN–GFP (indicating a PIP_2-rich membrane) remained constant on the membrane that was shielded against extracellular cAMP. The localization of PTEN thus exhibited an inverted pattern as compared with the localization of PH_{CRAC}–GFP and actin. In summary, our findings indicate that localized stimulation of the signal transduction pathway from the cAMP receptor to the actin machinery, including the PIP_3/PIP_2 system and filamentous actin, does not trigger excitations that

Journal of Cell Science (2014) 127, 5115–5125 doi:10.1242/jcs.161133

autonomously spread across the membrane. Only those parts of the membrane that are in direct contact with extracellular cAMP remain in the excited state (Fig. 8A).

Earlier work has shown that *Dictyostelium* cells might exhibit dynamic wave patterns involving PI3K and PTEN activity as well actin polymerization (Gerisch et al., 2004; Bretschneider et al., 2009). They emerge independently of any receptor input signal and propagate as composite structures over large distances across the substrate-attached cell membrane, displaying characteristic features of excitable waves (Taniguchi et al., 2013; Gerhardt et al., 2014). We assume that the receptor-independent positive-feedback circuit that has been reported in Gβγ-null cells and involves the spontaneous activation of Ras, PI3K and F-actin might provide the mechanistic bases for such spontaneously emerging wave patterns (Sasaki et al., 2007). In particular, as Ras and PI3K are activated immediately following a cAMP receptor signal, we expected that excitable waves should be initiated by a localized receptor stimulus. However, our present results indicate that this is not the case. No wave-like spreading of excitations was observed in response to a localized cAMP stimulus.

We point out that the absence of wave-like spreading in our experiments cannot be attributed to the choice of concentration of the external cAMP stimulus. Even though the cAMP concentration in the micro-pipette aspiration experiments was chosen such that a final concentration of 20 µM was reached in the well-mixed case, the initial cAMP exposure of the cells was much lower. This is due to the way in which the experiments were performed. We imaged cells that were attached to the bottom plate of a glass-bottomed Petri dish, covered by a layer of phosphate buffer with a total volume of ~1 ml. For stimulation, 20 µl of 1 mM cAMP solution was added with a micropipette. However, in order to avoid strong convection and disturbances of the cells in the field of view, the cAMP was not added directly to the cells in the field of view but at a distance of 1 cm away. From there, it spread into the dish by gentle convection and diffusion. The initial cAMP stimulus that the cells received was thus well below the final 20 µM that was only reached in the well-mixed case. In the supplementary material Movies 1 and 2, we display examples of cells that show spontaneous PIP_3 signaling on their membrane. When stimulating these cells according to the protocol described above, the cAMP response was comparable in strength to the initial autonomous signaling. The autonomous signaling activity was weakened by the receptor stimulus but typically re-emerged after the response to the uniform cAMP stimulus had decayed. We thus conclude that the actual receptor stimulus was strong but still within the physiological range, where native signaling activities of the cells take place. No cringing responses or other effects that might indicate massive cAMP exposure were observed. By contrast, these cAMP concentrations ensure that we are not operating in the subthreshold regime of this receptor-mediated signaling system.

Our findings suggest that a uniform cAMP stimulus transiently weakens the autonomous signaling activity throughout the cell. In particular, a locally confined cAMP stimulus does not initiate the excitatory spatial spreading of the PI3K and F-actin activity along the membrane. Possible candidates that might suppress spatial excitability are the Gα and Gβγ subclusters that are released by the cAMP receptor upon ligand binding. This hypothesis is supported by the fact that the class 1b PI3K shows a binding site for Gβγ in mammalian cells (Krugmann et al., 2002; Brock et al., 2003; Suire et al., 2005). Direct interaction between the Gβγ subcluster and PI3K might alter the spatial spreading of excitations of the intrinsic PI3K–F-actin feedback system, keeping in mind that a membrane anchor has been reported for the Gβγ subcluster (Stephens et al., 1997; Brock et al., 2003).

In agreement with the reciprocal localization pattern of PI3K and PTEN in *Dictyostelium* cells exposed to cAMP gradients (Iijima and Devreotes, 2002; Funamoto et al., 2002), here we observed that PTEN–GFP accumulates in those membrane areas that are not decorated with the PIP_3-marker PH_{CRAC}–GFP. Hodakoski et al., 2014 reported that PIP_3-dependent Rac exchanger 2 (PREX2) can inhibit PTEN in mammalian cells. Even though it is not known whether a homolog exists in *Dictyostelium*, we can speculate that a PIP_3-dependent PTEN inactivator restricts PTEN activity to those membrane regions that do not contain PIP_3, so that PIP_3-rich membrane regions triggered by cAMP receptor stimuli remain stationary in space (see the schematic in Fig. 8B). Note that PREX2 might additionally depend on the Gβγ subunit, as has been reported for PREX1 (Welch et al., 2002).

Comparison to models of chemotactic gradient sensing

Our results are in line with common models of chemotactic gradient sensing based on the concept of LEGI (Parent and Devreotes, 1999; Levchenko and Iglesias, 2002). A slow-diffusing localized activator and a fast-diffusing inhibitor are

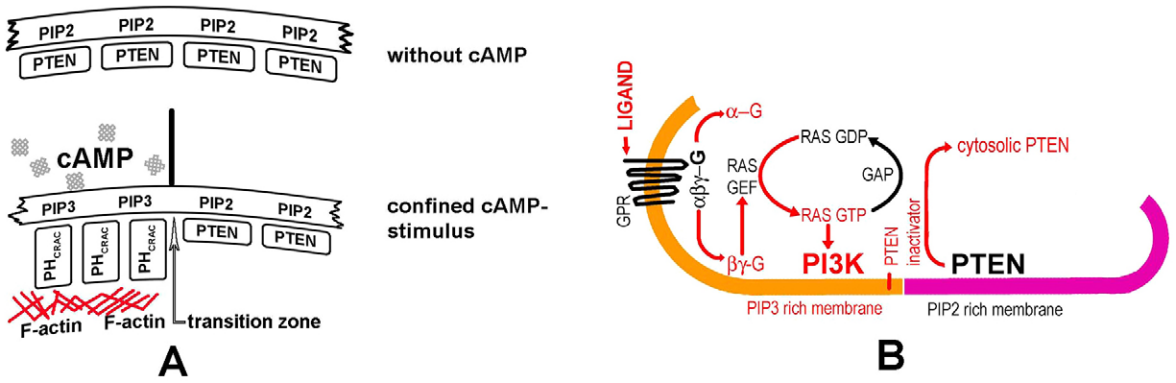

Fig. 8. Schematic view of the confined cAMP stimulus and of the signal transduction pathway. (A) Schematic view of the spatial distribution of filamentous actin, PIP_2, PIP_3, PTEN and PH_{CRAC} during extracellular cAMP stimulation of a confined membrane region. (B) Schematic view of the signaling pathway initiated by ligand binding to the GPR, leading to PI3K activation and PIP_3 synthesis. GPR, G-protein-associated receptor; PTEN, phosphatase and tensin homolog deleted on chromosome ten; PI3K, phosphoinositide 3-kinase; RAS GEF, Ras guanine exchange factor; GAP, GTPase activating protein; G, G protein.

Journal of Cell Science (2014) 127, 5115–5125 doi:10.1242/jcs.161133

released upon receptor binding and set a threshold, so that intracellular downstream signaling is triggered only at those parts of the membrane where the local concentration of the activator exceeds the inhibitor concentration. In this way, the LEGI model can explain how cells undergoing chemotaxis in a shallow cAMP gradient might undergo a strong symmetry breaking, such that PIP_3 is produced only at the side of the cell pointing towards the higher cAMP concentration. Similarly, the LEGI model can account for our observation that PIP_3 formation is confined to those membrane areas that are in direct contact with extracellular cAMP in a step-like concentration profile. In addition, the data from our stimulation experiments with cAMP-coated particles indicates that those parts of the cell membrane that are not in direct contact with the particle surface become less responsive to a subsequent cAMP stimulus (supplementary material Movies 3, 4). These observations support an underlying LEGI-type mechanism, where signaling activity is suppressed by a global inhibitor in those parts of the membrane that are not (or are to a lesser extent) excited by a chemoattractant stimulus. This is in line with the long durations of the localized signaling events, similar to translocation events initiated by shallower cAMP gradients.

Recently, LEGI-type gradient-sensing models have been combined with excitable modules in various ways to account for the dynamics of pseudopod formation during chemotactic motion. Xiong and colleagues have combined a LEGI-type compass model with excitable downstream cytoskeletal activity (Xiong et al., 2010). Huang and co-workers separate the signal transduction chain into an excitable part including Ras, PI3K and Rac on the one hand, and an oscillatory part that involves SCAR/WAVE, Arp2/3, coronin and actin on the other hand (Huang et al., 2013). In both cases, it is expected that stochastic fluctuations randomly trigger excitation waves that ultimately result in pseudopod formation. Gradient cues then lower the excitation threshold on one side of the cell, so that pseudopod formation is directionally biased, resulting in chemotactic movement.

In the light of our findings, we suggest the following overall picture. Excitability in the signaling system including Ras and PI3K/PTEN displays noise-induced spontaneous wave formation and random motility in the absence of external cues. Under spatially uniform receptor input signals, the temporal signatures of an excitable system are clearly conserved (Huang et al., 2013). However, in the presence of spatially non-uniform cAMP stimuli (gradients or step profiles), wave-like spreading of excitations is suppressed and the dynamics of the signaling system are well described by a LEGI-type compass model. This is in line with current views on the cellular functions associated with these dynamic structures. Although randomly initiated excitable wave patterns represent an efficient strategy to screen a substrate surface for nutrient particles to be taken up by phagocytosis (Gerisch et al., 2009), such wave patterns might not be optimal for directional locomotion. Instead, in the presence of non-uniform receptor stimuli (gradients of step profiles) the activity of the signaling pathway is confined to the activated membrane areas, where pseudopodia will be formed for efficient forward motion.

MATERIALS AND METHODS

Cell culture and imaging

We used *Dictyostelium discoideum* cell lines expressing (1) DdLimEΔ–RFP and PTEN–GFP in AX2, kindly provided by Günther Gerisch (Martinsried, Germany; Gerisch et al., 2012) and (2) PH_{CRAC}–GFP in AX3, kindly provided by Peter N. Devreotes (Johns Hopkins University, Baltimore, MD). Both cell lines were grown in HL5 medium (Foremedium) containing (1) 5 µg/ml blasticidin, 10 µg/ml geneticin and 33 µg/ml hygromycin B and (2) 0.5 µg/ml geneticin. The optical density of the cell cultures was continuously recorded to identify the best point in time for harvesting the cells during the exponential growth phase. At this point, the cell density reached $\sim 2\times10^6$ cells/ml. The cells were harvested by centrifugation (at 300 ***g*** for 3 min) and washed once in phosphate buffer (2.1 mM Na_2HPO_4, 14.6 mM KH_2PO_4, 2 mM $CaCl_2$ in 0.05 µS/cm water). Finally, the cells were equilibrated at a density of 2×10^6 cells/ml in phosphate buffer for differentiation. The cells were differentiated by starvation in a shaking flask culture at 150 rpm for 4–5 h and exposed to periodic pulses of cAMP (one every 6 min, 50 nM final concentration) using a computer-controlled pump.

Cells were imaged by laser-scanning confocal microscopy at excitation wavelengths of 488 nm and 526 nm (simultaneously for GFP and RFP) with a resolution of 1024×1024 pixels per image using an LSM780 microscope (Zeiss, Germany) equipped with a PlanApo 40×/NA 1.4 oil objective. Prior to each experiment, a sample from the shaking culture was exposed to a uniform stimulus of 20 µM cAMP (final concentration), and the translocation of the fluorescent markers in response to the stimulus was recorded. If a translocation was clearly detectable (membrane recruitment of PH_{CRAC}–GFP, or membrane recruitment of DdLimEΔ–RFP followed by restoration of the PTEN–GFP decoration) the cells were considered ready for further experiments.

Particle-based cAMP stimulation

Sepharose particles decorated with surface-immobilized cAMP molecules were obtained from Biolog GmbH, Bremen, Germany. Particles with four different linker configurations were used: (1) 8-AH-cAMP [8-(6-aminohexylamino)-adenosine-3′,5′-cyclic monophosphate]; (2) 6-AH-cAMP [N6-(6-aminohexyl)-adenosine-3′,5′-cyclic monophosphate]; (3) 2-AH-cAMP [2-(6-aminohexylamino)-adenosine-3′,5′-cyclic monophosphate]; (4) 2′O-AHC-cAMP [2′-O-(6-aminohexylcarbamoyl)-adenosine-3′,5′-cyclic monophosphate]. For chemical structures see supplementary material Fig. S1. Differentiated cells were brought into contact with cAMP particles either by letting the particles sediment onto the cells or by controlled movement. In the latter case, a particle was impaled on a glass micropipette that was mounted on a micromanipulator. Using the micromanipulator, the impaled cAMP particle was gently lowered to come into contact with a selected cell in a well-controlled fashion. For better visibility, the surface of the particles was stained with Rhodamine, kindly provided by Bernd-Reiner Paulke (Fraunhofer IBMT Potsdam, Germany). During collision, the impaled cAMP-coated particle and the cell were continuously imaged by laser-scanning confocal microscopy in the *Z*-stack scan mode, simultaneously exciting at 488 nm and 526 nm using a LSM710 microscope (Zeiss, Germany) equipped with a PlanApo 40×/NA 1.4 oil objective and a micromanipulator.

Patch clamp shielding

Confined cAMP stimuli were generated by shielding a patch of the cell membrane in a glass pipette during exposure of the cell to extracellular cAMP. Pipettes were manufactured using a pipette puller, such that the tip opening was between 2 and 3 µm (Zeitz Instruments, Germany or Sutter Instruments, CA). With the help of a micromanipulator, the open tip of the glass pipette was moved close to the membrane of a differentiated cell and a patch of its membrane was aspirated into the pipette by applying negative pressure. To monitor the seal between the membrane patch inside the pipette and the extracellular medium, an Axopatch 200B amplifier (Molecular Devices Inc., CA) in combination with an oscilloscope and a square-wave generator was used. If the seal resistivity showed a value >50 MΩ, the membrane patch was considered to be sealed against the extracellular space. The membrane patch inside the pipette and the remaining part of the cell outside were imaged by laser-scanning confocal microscopy as described above.

Image analysis

We developed an image analysis algorithm to quantify the average intracellular membrane decoration with fluorescent markers. In a first step, the perimeter of a chosen cell was automatically rendered as an

n-degree polygon with a point-to-point distance of 5 pixels. At each point of the polygon, the fluorescence profile was measured over a length of 4 µm normal to the cell border. We then averaged the intensity profiles obtained for all points of the polygon to obtain an average intensity profile across the cell membrane.

Acknowledgements
We thank Günther Gerisch (MPI Martinsried, Germany) for providing *Dictyostelium* cell lines, Kirsten Krüger (Institute of Physics and Astronomy, University of Potsdam, Germany) for cell culture support, and Bernd-Reiner Paulke (Fraunhofer IBMT Potsdam, Germany) for providing Rhodamine-coated nanoparticles. Additionally we thank Otto Baumann (Institute of Biochemistry and Biology, University of Potsdam, Germany) for fruitful discussions and Frank Schwede (Biolog GmbH, Germany) for information on the cAMP-coated Sepharose particles.

Competing interests
The authors declare no competing interests.

Author contributions
M.G. and M.W. performed experiments and analyzed data. M.G. and C.B. designed the research project, evaluated the results and wrote the paper.

Funding
This work was supported by the University of Potsdam ('Einzelförderung für Postdocs, Personal- und Sachmittel' to M.G.); by the Ministerium für Wissenschaft, Forschung und Kultur des Landes Brandenburg together with the Europäische Fond für Regionalentwicklung ('Hochschulinvestitionsprogramm') [grant number 80139590 to C.B.]; and by the Deutsche Forschungsgemeinschaft [grant number BE 3978/3-1 to C.B.].

Supplementary material
Supplementary material available online at
http://jcs.biologists.org/lookup/suppl/doi:10.1242/jcs.161133/-/DC1

References
Annesley, S. J. and Fisher, P. R. (2009). Dictyostelium discoideum – a model for many reasons. *Mol. Cell. Biochem.* **329**, 73-91.
Beta, C., Amselem, G. and Bodenschatz, E. (2008). A bistable mechanism for directional sensing. *New J. Phys.* **10**, 083015.
Bretschneider, T., Anderson, K., Ecke, M., Müller-Taubenberger, A., Schroth-Diez, B., Ishikawa-Ankerhold, H. C. and Gerisch, G. (2009). The three-dimensional dynamics of actin waves, a model of cytoskeletal self-organization. *Biophys. J.* **96**, 2888-2900.
Brock, C., Schaefer, M., Reusch, H. P., Czupalla, C., Michalke, M., Spicher, K., Schultz, G. and Nürnberg, B. (2003). Roles of G beta gamma in membrane recruitment and activation of p110 gamma/p101 phosphoinositide 3-kinase gamma. *J. Cell Biol.* **160**, 89-99.
Cooper, R. M., Wingreen, N. S. and Cox, E. C. (2012). An excitable cortex and memory model successfully predicts new pseudopod dynamics. *PLoS ONE* **7**, e33528.
Elzie, C. A., Colby, J., Sammons, M. A. and Janetopoulos, C. (2009). Dynamic localization of G proteins in Dictyostelium discoideum. *J. Cell Sci.* **122**, 2597-2603.
Friedl, P. and Gilmour, D. (2009). Collective cell migration in morphogenesis, regeneration and cancer. *Nat. Rev. Mol. Cell Biol.* **10**, 445-457.
Funamoto, S., Meili, R., Lee, S., Parry, L. and Firtel, R. A. (2002). Spatial and temporal regulation of 3-phosphoinositides by PI 3-kinase and PTEN mediates chemotaxis. *Cell* **109**, 611-623.
Gerhardt, M., Groeger, G. and Maccarthy, N. (2011). Monopolar vs. bipolar subretinal stimulation-an in vitro study. *J. Neurosci. Methods* **199**, 26-34.
Gerhardt, M., Ecke, M., Walz, M., Stengl, A., Beta, C. and Gerisch, G. (2014). Actin and PIP3 waves in giant cells reveal the inherent length scale of an excited state. *J. Cell Sci.* **127**, 4507-4517.
Gerisch, G., Bretschneider, T., Müller-Taubenberger, A., Simmeth, E., Ecke, M., Diez, S. and Anderson, K. (2004). Mobile actin clusters and traveling waves in cells recovering from actin depolymerization. *Biophys. J.* **87**, 3493-3503.
Gerisch, G., Ecke, M., Schroth-Diez, B., Gerwig, S., Engel, U., Maddera, L. and Clarke, M. (2009). Self-organizing actin waves as planar phagocytic cup structures. *Cell Adh. Migr.* **3**, 373-382.
Gerisch, G., Ecke, M., Wischnewski, D. and Schroth-Diez, B. (2011). Different modes of state transitions determine pattern in the Phosphatidylinositide-Actin system. *BMC Cell Biol.* **12**, 42.
Gerisch, G., Schroth-Diez, B., Müller-Taubenberger, A. and Ecke, M. (2012). PIP3 waves and PTEN dynamics in the emergence of cell polarity. *Biophys. J.* **103**, 1170-1178.
Hecht, I., Skoge, M. L., Charest, P. G., Ben-Jacob, E., Firtel, R. A., Loomis, W. F., Levine, H. and Rappel, W.-J. (2011). Activated membrane patches guide chemotactic cell motility. *PLOS Comput. Biol.* **7**, e1002044.
Hodakoski, C., Hopkins, B. D., Barrows, D., Mense, S. M., Keniry, M., Anderson, K. E., Kern, P. A., Hawkins, P. T., Stephens, L. R. and Parsons, R. (2014). Regulation of PTEN inhibition by the pleckstrin homology domain of P-REX2 during insulin signaling and glucose homeostasis. *Proc. Natl. Acad. Sci. USA* **111**, 155-160.
Hoeller, O. and Kay, R. R. (2007). Chemotaxis in the absence of PIP3 gradients. *Curr. Biol.* **17**, 813-817.
Huang, C.-H., Tang, M., Shi, C., Iglesias, P. A. and Devreotes, P. N. (2013). An excitable signal integrator couples to an idling cytoskeletal oscillator to drive cell migration. *Nat. Cell Biol.* **15**, 1307-1316.
Iijima, M. and Devreotes, P. (2002). Tumor suppressor PTEN mediates sensing of chemoattractant gradients. *Cell* **109**, 599-610.
Insall, R. H., Soede, R. D., Schaap, P. and Devreotes, P. N. (1994). Two cAMP receptors activate common signaling pathways in Dictyostelium. *Mol. Biol. Cell* **5**, 703-711.
Janetopoulos, C., Jin, T. and Devreotes, P. (2001). Receptor-mediated activation of heterotrimeric G-proteins in living cells. *Science* **291**, 2408-2411.
Kae, H., Kortholt, A., Rehmann, H., Insall, R. H., Van Haastert, P. J., Spiegelman, G. B. and Weeks, G. (2007). Cyclic AMP signalling in Dictyostelium: G-proteins activate separate Ras pathways using specific RasGEFs. *EMBO Rep.* **8**, 477-482.
Kataria, R., Xu, X., Fusetti, F., Keizer-Gunnink, I., Jin, T., van Haastert, P. J. M. and Kortholt, A. (2013). Dictyostelium Ric8 is a nonreceptor guanine exchange factor for heterotrimeric G proteins and is important for development and chemotaxis. *Proc. Natl. Acad. Sci. USA* **110**, 6424-6429.
Knoch, F., Tarantola, M., Bodenschatz, E. and Rappel, W.-J. (2014). Modeling self-organized spatio-temporal patterns of PIP_3 and PTEN during spontaneous cell polarization. *Phys. Biol.* **11**, 046002.
Kölsch, V., Charest, P. G. and Firtel, R. A. (2008). The regulation of cell motility and chemotaxis by phospholipid signaling. *J. Cell Sci.* **121**, 551-559.
Kortholt, A., Keizer-Gunnink, I., Kataria, R. and Haastert, P. J. M. V. (2013). Ras activation and symmetry breaking during Dictyostelium chemotaxis. *J. Cell. Sci.* **126**, 4502-4513.
Krugmann, S., Cooper, M. A., Williams, D. H., Hawkins, P. T. and Stephens, L. R. (2002). Mechanism of the regulation of type IB phosphoinositide 3OH-kinase byG-protein betagamma subunits. *Biochem. J.* **362**, 725-731.
Levchenko, A. and Iglesias, P. A. (2002). Models of eukaryotic gradient sensing: application to chemotaxis of amoebae and neutrophils. *Biophys. J.* **82**, 50-63.
Levine, H., Kessler, D. A. and Rappel, W.-J. (2006). Directional sensing in eukaryotic chemotaxis: a balanced inactivation model. *Proc. Natl. Acad. Sci. USA* **103**, 9761-9766.
Luo, T., Mohan, K., Iglesias, P. A. and Robinson, D. N. (2013). Molecular mechanisms of cellular mechanosensing. *Nat. Mater.* **12**, 1064-1071.
Mato, J. M., Jastorff, B., Morr, M. and Konijn, T. M. (1978). A model for cyclic AMP-chemoreceptor interaction in Dictyostelium discoideum. *Biochim. Biophys. Acta* **544**, 309-314.
Neilson, M. P., Veltman, D. M., van Haastert, P. J. M., Webb, S. D., Mackenzie, J. A. and Insall, R. H. (2011). Chemotaxis: a feedback-based computational model robustly predicts multiple aspects of real cell behaviour. *PLoS Biol.* **9**, e1000618.
Nishikawa, M., Hörning, M., Ueda, M. and Shibata, T. (2014). Excitable signal transduction induces both spontaneous and directional cell asymmetries in the phosphatidylinositol lipid signaling system for eukaryotic chemotaxis. *Biophys. J.* **106**, 723-734.
Pantaloni, D., Le Clainche, C. and Carlier, M. F. (2001). Mechanism of actin-based motility. *Science* **292**, 1502-1506.
Parent, C. A. and Devreotes, P. N. (1999). A cell's sense of direction. *Science* **284**, 765-770.
Parent, C. A., Blacklock, B. J., Froehlich, W. M., Murphy, D. B. and Devreotes, P. N. (1998). G protein signaling events are activated at the leading edge of chemotactic cells. *Cell* **95**, 81-91.
Postma, M., Roelofs, J., Goedhart, J., Loovers, H. M., Visser, A. J. W. G. and Van Haastert, P. J. (2004). Sensitization of Dictyostelium chemotaxis by phosphoinositide-3-kinase-mediated self-organizing signalling patches. *J. Cell Sci.* **117**, 2925-2935.
Prabhu, Y. and Eichinger, L. (2006). The Dictyostelium repertoire of seven transmembrane domain receptors. *Eur. J. Cell Biol.* **85**, 937-946.
Rahdar, M., Inoue, T., Meyer, T., Zhang, J., Vazquez, F. and Devreotes, P. N. (2009). A phosphorylation-dependent intramolecular interaction regulates the membrane association and activity of the tumor suppressor PTEN. *Proc. Natl. Acad. Sci. USA* **106**, 480-485.
Ridley, A. J., Schwartz, M. A., Burridge, K., Firtel, R. A., Ginsberg, M. H., Borisy, G., Parsons, J. T. and Horwitz, A. R. (2003). Cell migration: integrating signals from front to back. *Science* **302**, 1704-1709.
Sasaki, A. T., Chun, C., Takeda, K. and Firtel, R. A. (2004). Localized Ras signaling at the leading edge regulates PI3K, cell polarity, and directional cell movement. *J. Cell Biol.* **167**, 505-518.
Sasaki, A. T., Janetopoulos, C., Lee, S., Charest, P. G., Takeda, K., Sundheimer, L. W., Meili, R., Devreotes, P. N. and Firtel, R. A. (2007). G protein-independent Ras/PI3K/F-actin circuit regulates basic cell motility. *J. Cell Biol.* **178**, 185-191.
Schneider, N., Weber, I., Faix, J., Prassler, J., Müller-Taubenberger, A., Köhler, J., Burghardt, E., Gerisch, G. and Marriott, G. (2003). A Lim protein involved in the progression of cytokinesis and regulation of the mitotic spindle. *Cell Motil. Cytoskeleton* **56**, 130-139.

Stein, R. C. and Waterfield, M. D. (2000). PI3-kinase inhibition: a target for drug development? *Mol. Med. Today* **6**, 347-358.
Stephens, L. R., Eguinoa, A., Erdjument-Bromage, H., Lui, M., Cooke, F., Coadwell, J., Smrcka, A. S., Thelen, M., Cadwallader, K., Tempst, P. et al. (1997). The G beta gamma sensitivity of a PI3K is dependent upon a tightly associated adaptor, p101. *Cell* **89**, 105-114.
Stett, A., Barth, W., Weiss, S., Haemmerle, H. and Zrenner, E. (2000). Electrical multisite stimulation of the isolated chicken retina. *Vision Res.* **40**, 1785-1795.
Suire, S., Coadwell, J., Ferguson, G. J., Davidson, K., Hawkins, P. and Stephens, L. (2005). p84, a new Gbetagamma-activated regulatory subunit of the type IB phosphoinositide 3-kinase p110gamma. *Curr. Biol.* **15**, 566-570.
Swaney, K. F., Huang, C.-H. and Devreotes, P. N. (2010). Eukaryotic chemotaxis: a network of signaling pathways controls motility, directional sensing, and polarity. *Annu. Rev. Biophys.* **39**, 265-289.
Takeda, K., Sasaki, A. T., Ha, H., Seung, H.-A. and Firtel, R. A. (2007). Role of phosphatidylinositol 3-kinases in chemotaxis in Dictyostelium. *J. Biol. Chem.* **282**, 11874-11884.
Takeda, K., Shao, D., Adler, M., Charest, P. G., Loomis, W. F., Levine, H., Groisman, A., Rappel, W.-J. and Firtel, R. A. (2012). Incoherent feedforward control governs adaptation of activated ras in a eukaryotic chemotaxis pathway. *Sci. Signal.* **5**, ra2.
Taniguchi, D., Ishihara, S., Oonuki, T., Honda-Kitahara, M., Kaneko, K. and Sawai, S. (2013). Phase geometries of two-dimensional excitable waves govern self-organized morphodynamics of amoeboid cells. *Proc. Natl. Acad. Sci. USA* **110**, 5016-5021.
Van Haastert, P. J. and Kien, E. (1983). Binding of cAMP derivatives to Dictyostelium discoideum cells. Activation mechanism of the cell surface cAMP receptor. *J. Biol. Chem.* **258**, 9636-9642.
Van Haastert, P. J., Jastorff, B., Pinas, J. E. and Konijn, T. M. (1982). Analogs of cyclic AMP as chemoattractants and inhibitors of Dictyostelium chemotaxis. *J. Bacteriol.* **149**, 99-105.
Welch, H. C. E., Coadwell, W. J., Ellson, C. D., Ferguson, G. J., Andrews, S. R., Erdjument-Bromage, H., Tempst, P., Hawkins, P. T. and Stephens, L. R. (2002). P-Rex1, a PtdIns(3,4,5)P3- and Gbetagamma-regulated guanine-nucleotide exchange factor for Rac. *Cell* **108**, 809-821.
Westendorf, C., Negrete, J., Jr, Bae, A. J., Sandmann, R., Bodenschatz, E. and Beta, C. (2013). Actin cytoskeleton of chemotactic amoebae operates close to the onset of oscillations. *Proc. Natl. Acad. Sci. USA* **110**, 3853-3858.
Xiong, Y., Huang, C.-H., Iglesias, P. A. and Devreotes, P. N. (2010). Cells navigate with a local-excitation, global-inhibition-biased excitable network. *Proc. Natl. Acad. Sci. USA* **107**, 17079-17086.
Xu, X., Meier-Schellersheim, M., Jiao, X., Nelson, L. E. and Jin, T. (2005). Quantitative imaging of single live cells reveals spatiotemporal dynamics of multistep signaling events of chemoattractant gradient sensing in Dictyostelium. *Mol. Biol. Cell* **16**, 676-688.

Supplementary Material

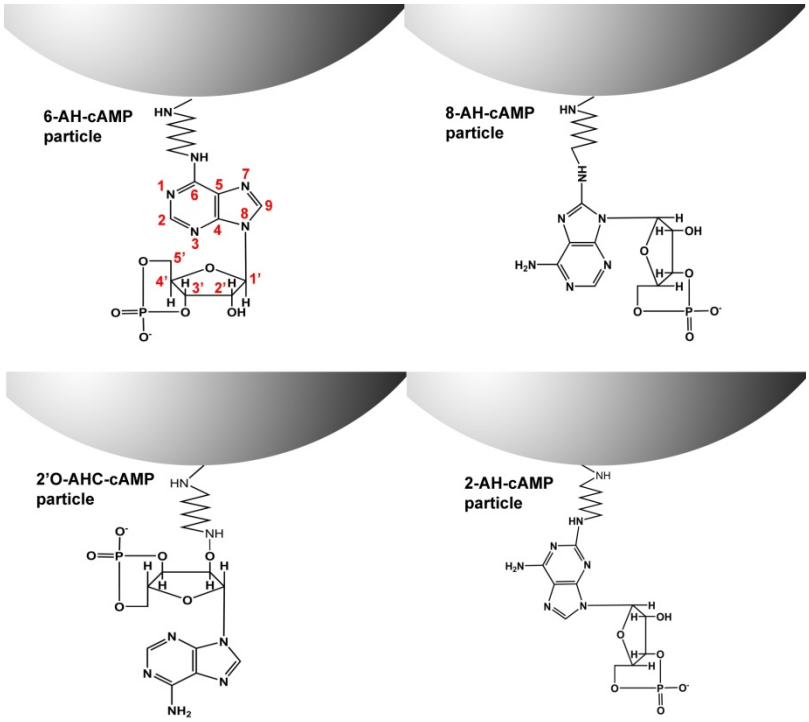

Fig. S1. Particles used to stimulate differentiated *Dictyostelium* cells with immobilized cAMP molecules. 8-AH-cAMP: 8-(6-aminohexylamino)-adenosine-3',5'-cyclomonophosphate; 6-AH-cAMP: N6-(6-aminohexyl)-adenosin-3', 5'-cyclomonophosphate; 2-AH-cAMP: 2-(6-aminohexylamino)-adenosin-3', 5'-cyclomonophosphate; 2'O-AHC-cAMP: 2'-O-(6-aminohexylcarbamoyl)-adenosine-3',5'-cyclomonophosphate.

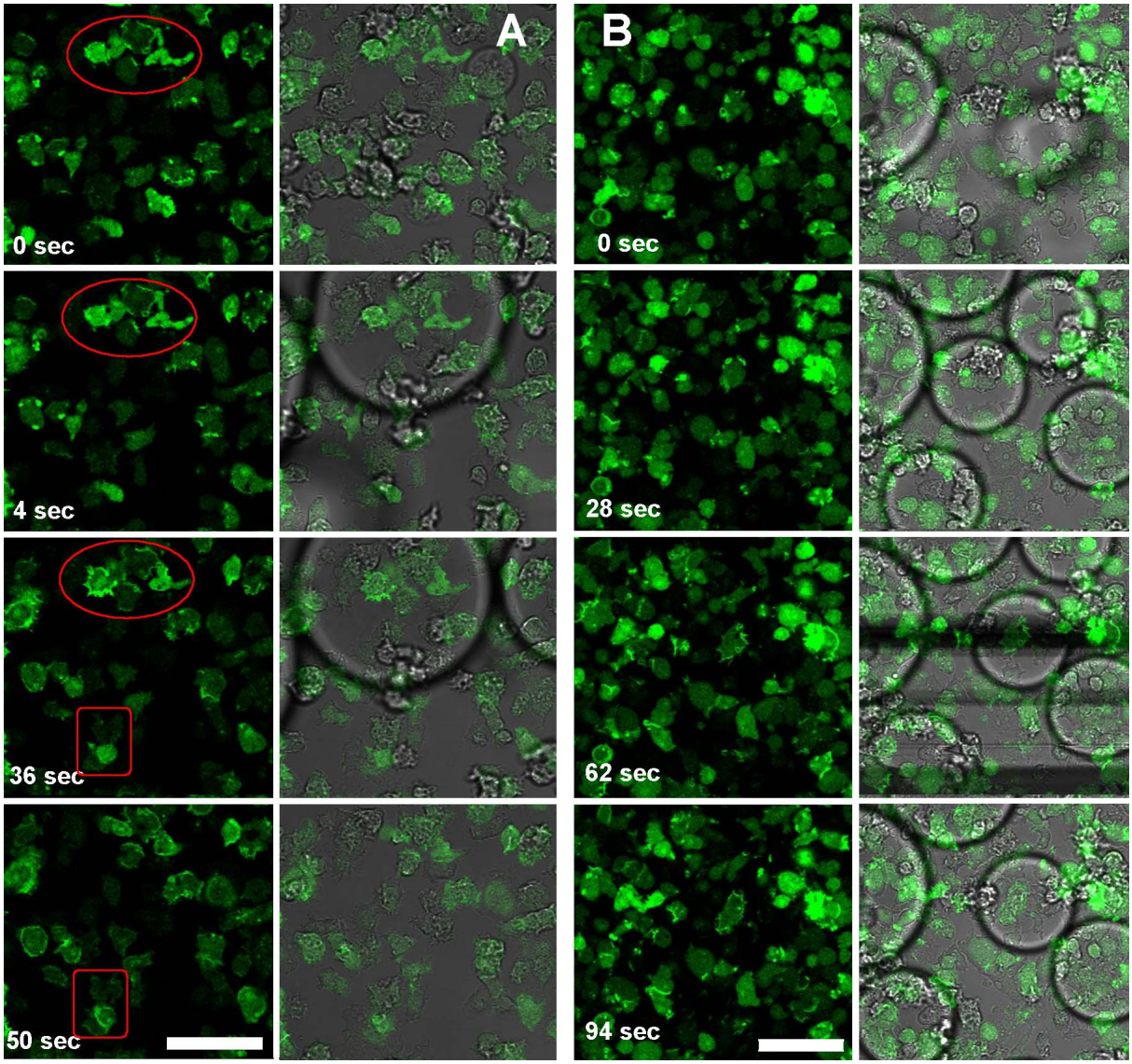

Fig. S2. Particles that expose 6-AH-cAMP (A) and 2'O-AHC-cAMP (B) where let to sediment on to a layer of differentiated *Dictyostelium* cells expressing the PIP3 marker PH_{CRAC}-GFP. (A) The green fluorescence of the marker increased in the membrane of such cells that were hit by the 6-AH-cAMP particles at a frame time of 4sec and indicates there for the presence of PIP3. Cells that had not been in contact with particles (red rectangle) did not display translocations of the marker indicated by no changes in the green fluorescence – only after 20 µM cAMP final were added at a frame time of 36 sec those cells also displayed an intracellular translocation of the marker which indicates for the presence of PIP3 in the membrane. (B) Upon collisions (7 - 24 sec) between the cells and 2'O-AHC-cAMP particles the intensity of green fluorescence did not changed. At a frame time of 62 sec 20 µM of cAMP final were added. Surprisingly also cells that had not been direct contact with the particles did not displayed any translocation of the marker intracellularly. Probably the presence of the 2'O-AHC-cAMP causes inhibition of the cAMP receptor causing no reaction in case of addition of free cAMP molecules. The size of the scale bar is 50 µm.

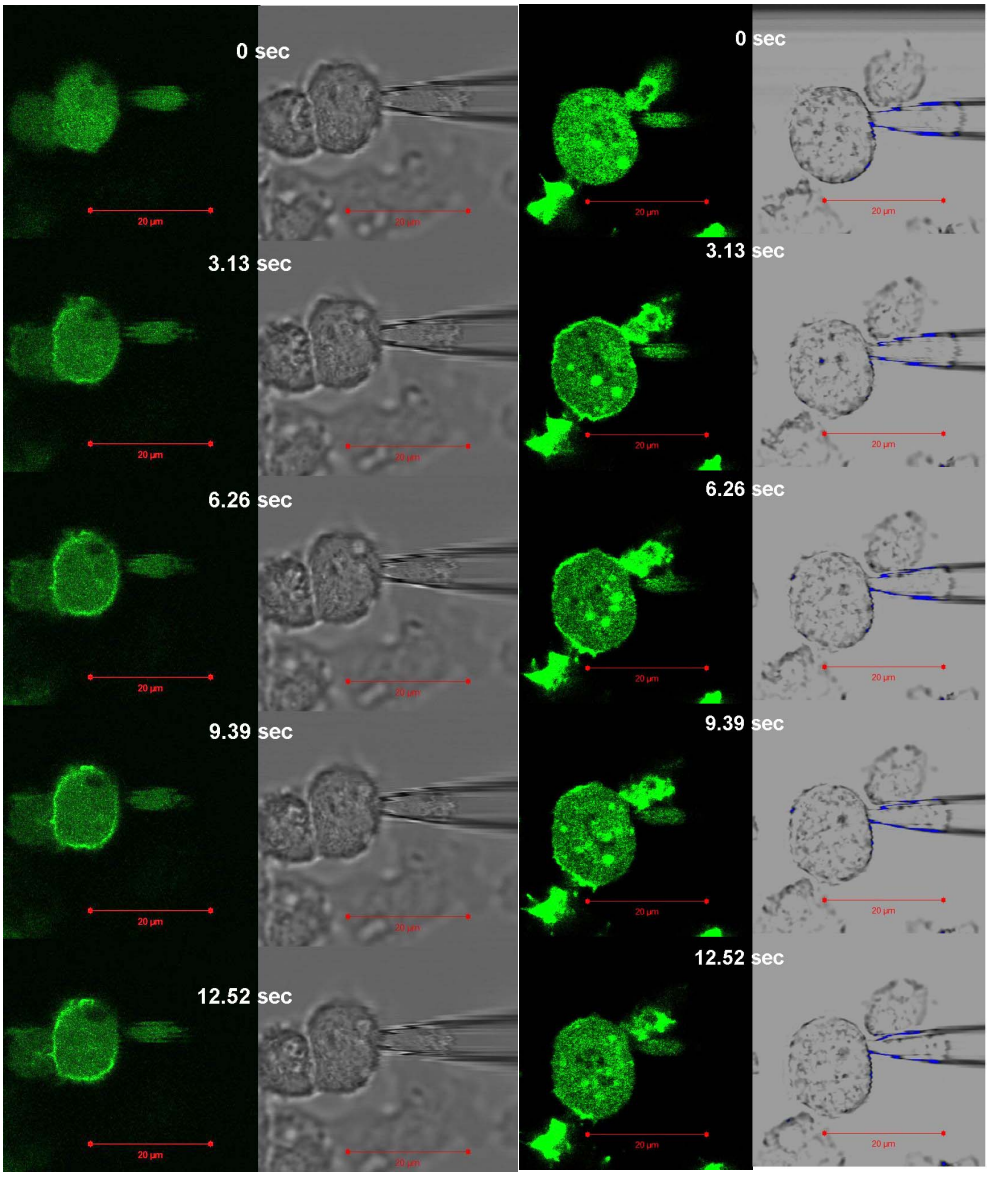

Fig. S3. Two examples of a shielding experiment, where a differentiated PH_{CRAC}-GFP expressing *Dictyostelium* cell is exposed to cAMP. A patch of the cell membrane was aspirated into the open tip of a glass micropipette and sealed with a seal resistivity higher than 50 MΩ by applying negative pressure. At a frame time of 0 sec, 20 µM cAMP final were added, which resulted in increased fluorescence intensity at the inner membrane while the fluorescence in the cytsol decreased. The fluorescence intensity in the aspirated patch stayed unchanged.

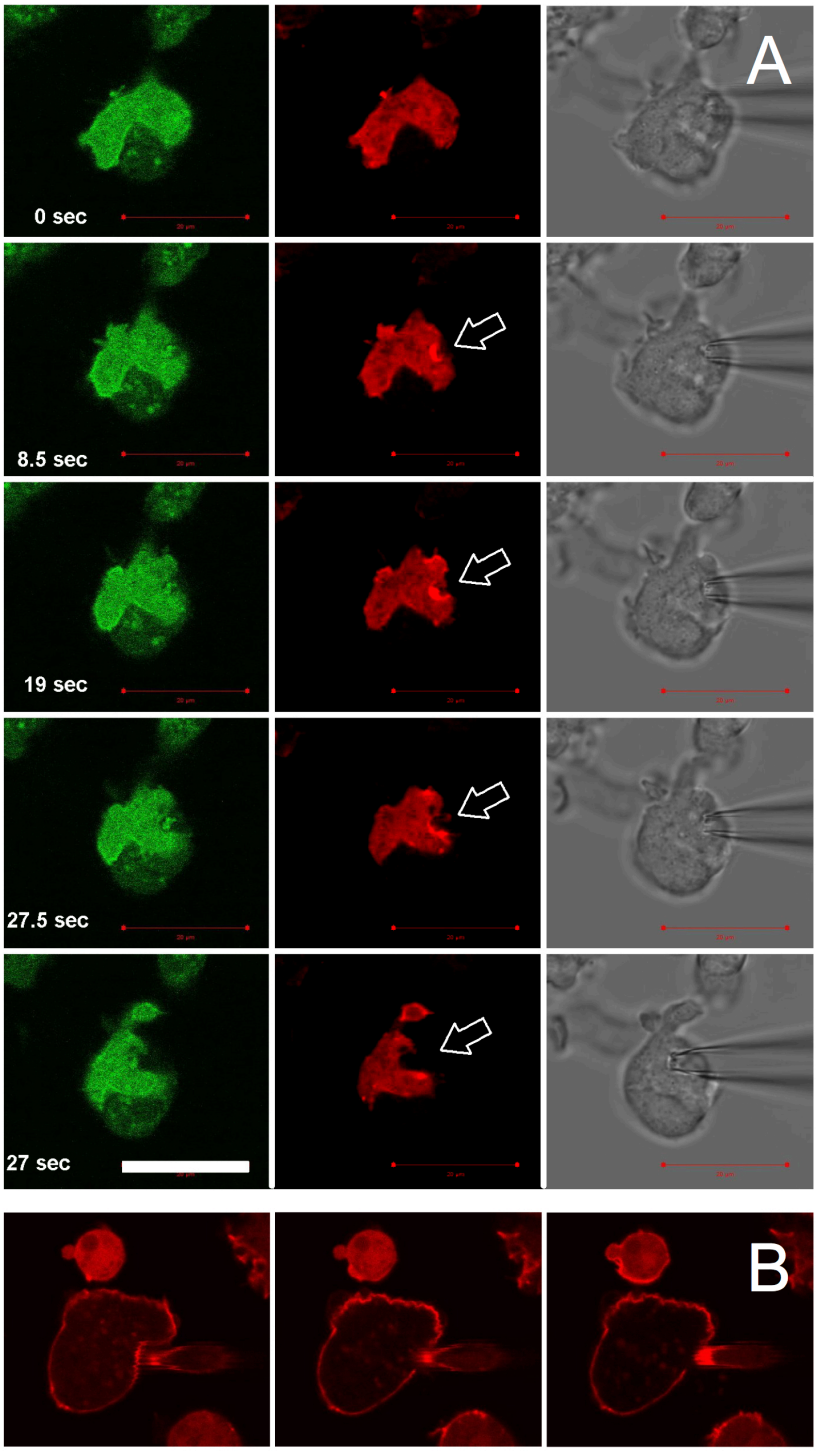

Fig. S4. Effects of mechanical stress. (A) Mechanical stimulation of a PTEN-GFP and DdLimEΔ-RFP coexpressing cell. Mechanical stress was induced by touching the surface of a differentiated cell with the tip of a glass pipette. The PTEN-GFP marker indicted no significant response of the cell whereas the fluorescence of the DdLimEΔ-RFP strongly increased at the membrane site in contact with the pipette tip (see arrow). After 28 sec, the DdLimEΔ-RFP fluorescence vanished, while the pipette tip was still in contact with the cell (scale bar 20 µm). (B) cAMP response of a DdLimEΔ-RFP expressing cell in the region of maximal mechanical stress. (left, middle) Cell with aspirated membrane patch before application of the cAMP stimulus. (right) Cell with aspirated membrane patch at the peak of the cAMP response. A strong LimEΔ translocation can be seen in the region of maximal mechanical stress.

Supplementary Movie Legends

Movie 1. Autonomous PIP3 signaling versus cAMP induced responses. PH_{CRAC}-GFP expressing cells are stimulated with 20 µM cAMP final (see the Discussion for a detailed concentration estimate). It can be seen that autonomous signaling exhibited by the cells prior to cAMP exposure is weakened but not wiped out by the cAMP stimulus (a cell displaying autonomous signaling is indicated by an arrow in the movie). The cAMP-triggered PH_{CRAC}-translocation is comparable in strength to the spontaneously occurring translocation patterns.

Movie 2. Autonomous PIP3 signaling versus cAMP induced responses. A second example for the same behavior, see caption of Movie 1 for further details.

Movie 3. Responsiveness of non-stimulated membrane areas to a subsequent cAMP stimulus. Example of a cell (indicated by a white arrow) in contact with a cAMP coated bead. The bead can be distinguished as a shadow in the bright field channel (a white outline is inserted during parts of the movie to guide the eye). Those parts of the cell membrane that did not touch the bead and thus did not exhibit any PIP3 signaling, are less responsive to a subsequent external cAMP stimulus. The cAMP stimulus can be observed indirectly through the response of the surrounding cells (indicated by yellow arrows).

Movie 4. Responsiveness of non-stimulated membrane areas to a subsequent cAMP stimulus. A second example for the same behavior, see caption of Movie 3 for further details. In addition, a red arrow points to the less responsive parts of the membrane.

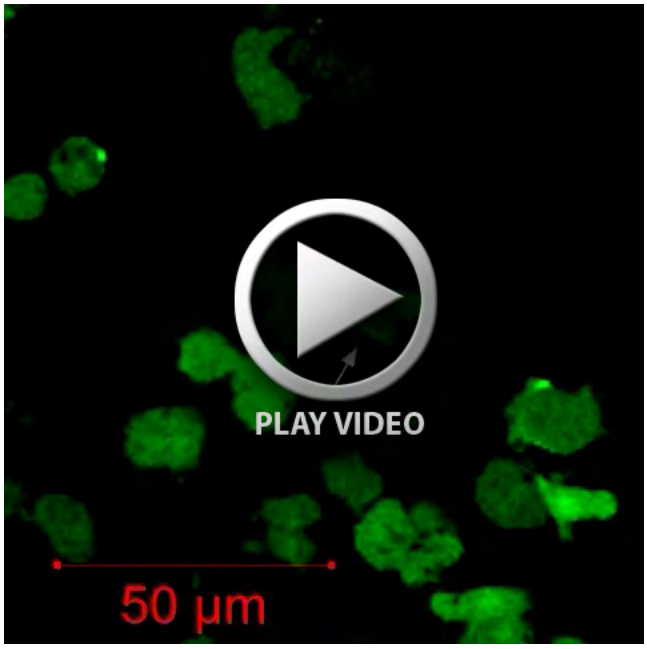

Movie 1.

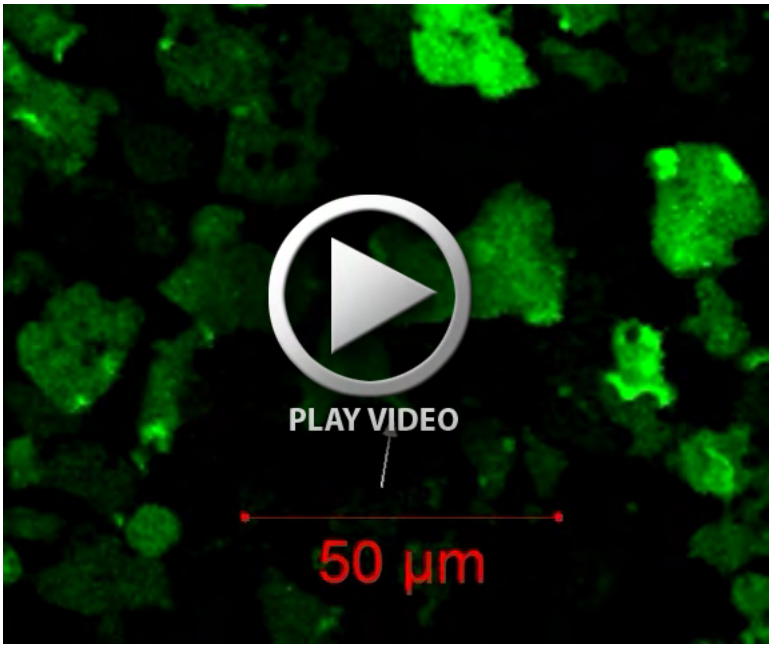

Movie 2.

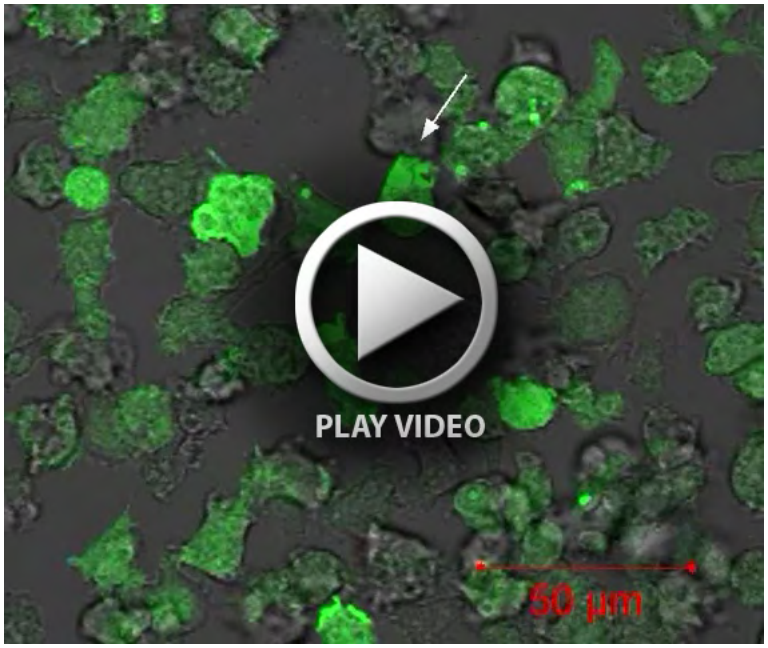

Movie 3.

Movie 4.